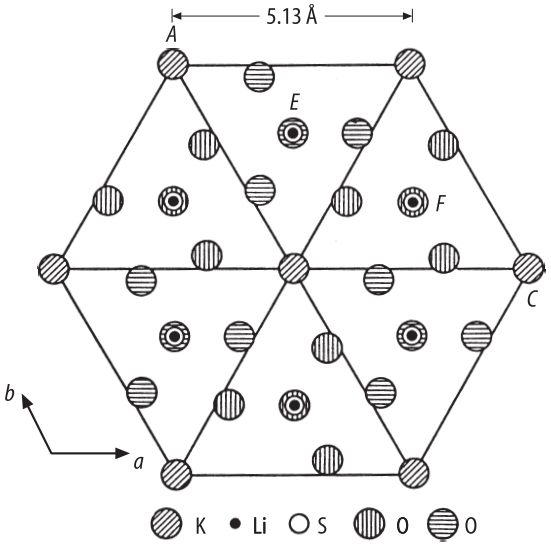

Fig. 41A-2-001. $KLiSO_4$. Projection of the crystal structure of phase IV at RT along the *c* axis [25Bra].

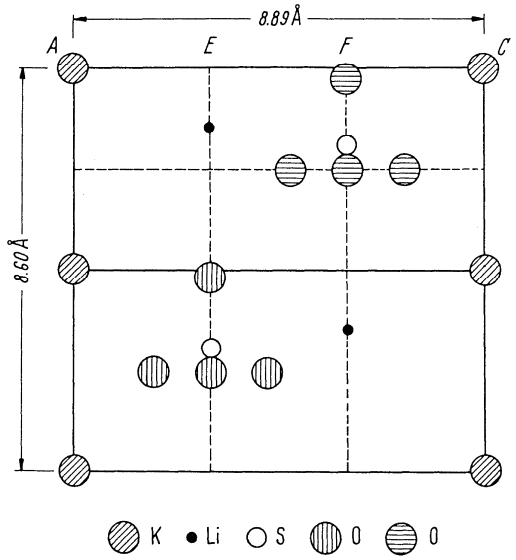

Fig. 41A-2-002. $KLiSO_4$. Projection of the crystal structure of phase IV at RT along $(1,0,\bar{1},0)$ [25Bra]. The letters *A*, *E*, *F*, *C* refer to the same position as in Fig. 41A-2-001.

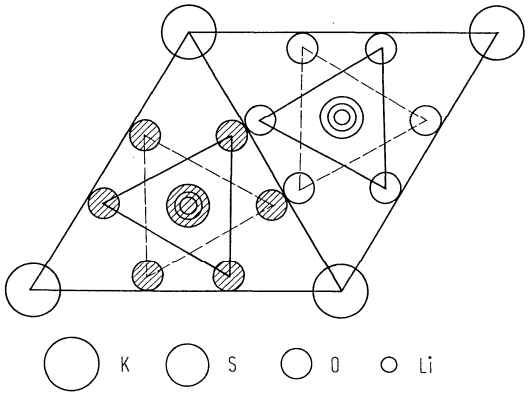

Fig. 41A-2-003. $KLiSO_4$. Structure of phase V [88Zha]. T = 200 K. View along c. The shaded circles are separated from open circles by $c/2$. The solid triangles and the dashed triangles represent the orientations of SO_4 tetrahedra, which form the twinning relation in the crystal.

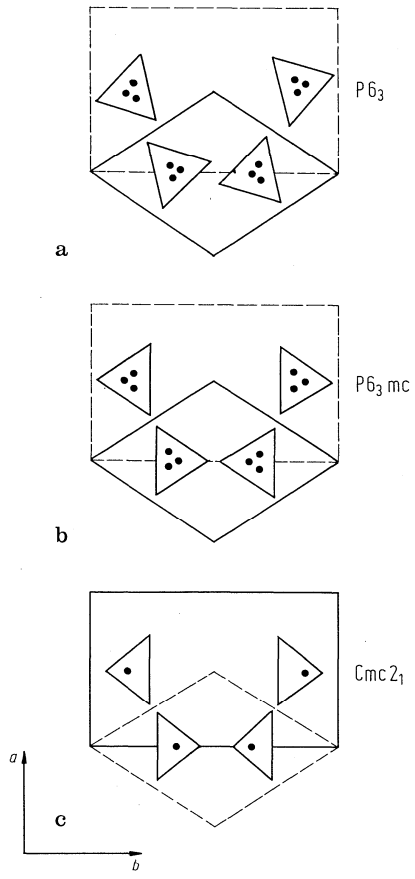

Fig. 41A-2-004. $KLiSO_4$. Structure [82Tom]. Schematic illustrations of the relation between hexagonal cell and orthorhombic cell. Triangles represent SO_4 tetrahedra. The top-oxygens of the tetrahedra are indicated by dots. Solid lines represent the true cell compatible with the space group. (**a**) Hexagonal cell of phase IV and pseudoorthorhombic cell. (**b**) Hexagonal cell of phase V and pseudoorthorhombic cell. (**c**) Orthorhombic cell of phase VI and pseudo-hexagonal cell.

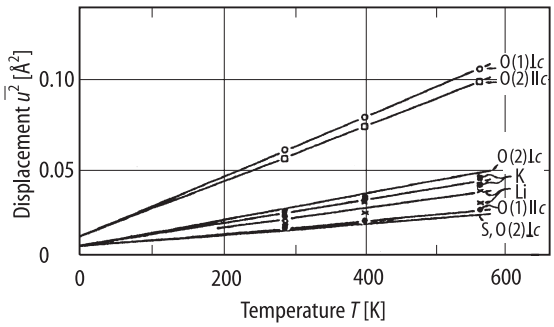

Fig. 41A-2-005. $KLiSO_4$. Structure of phase III and IV [85Shi]. Mean-square displacements vs. *T*.

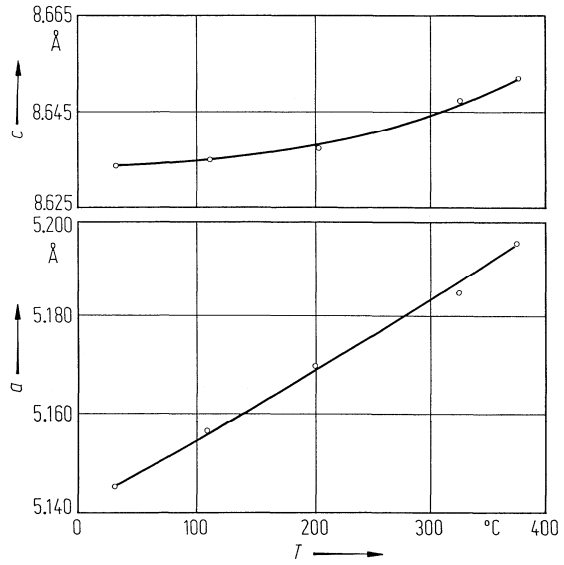

Fig. 41A-2-006. $KLiSO_4$. *a*, *c* vs. *T* [85Ven]. *a*, *c*: unit cell parameters.

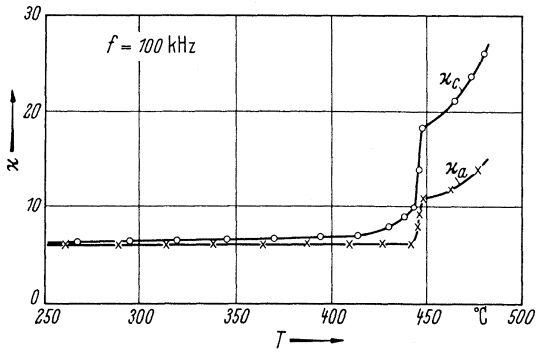

Fig. 41A-2-007. $KLiSO_4$. κ_a, κ_c vs. *T* [62And].

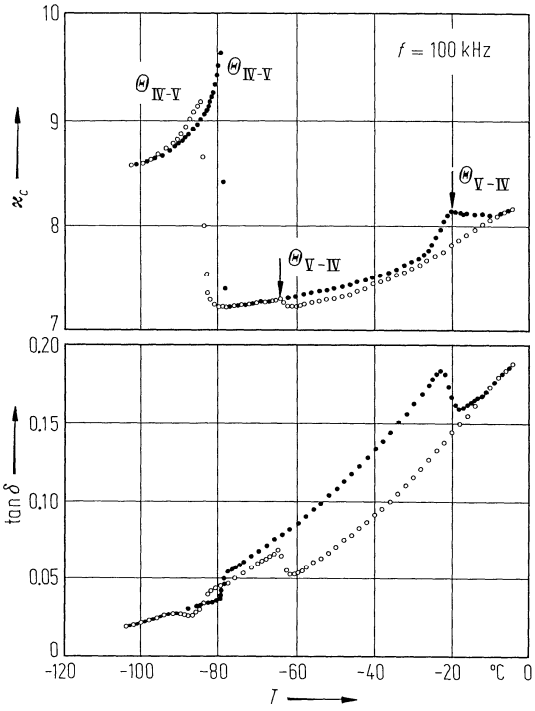

Fig. 41A-2-008. $KLiSO_4$. κ_c, $\tan\delta$ vs. T [85Fuj2]. Open circle: on cooling; full circle: on heating.

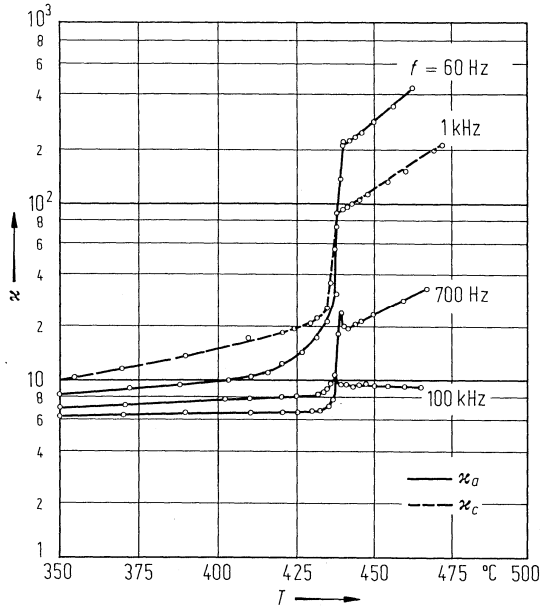

Fig. 41A-2-009. $KLiSO_4$. κ_a, κ_c vs. T [82Zhu]. Parameter: f.

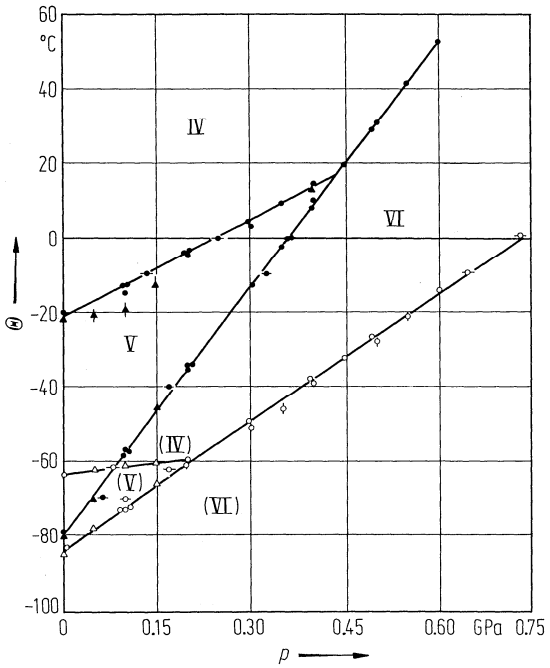

Fig. 41A-2-010. $KLiSO_4$. Θ vs. p [85Fuj1]. Closed marks: from measurement on heating or increasing pressure processes. Open marks: on cooling or decreasing pressure processes. Different marks show different types of measurements.

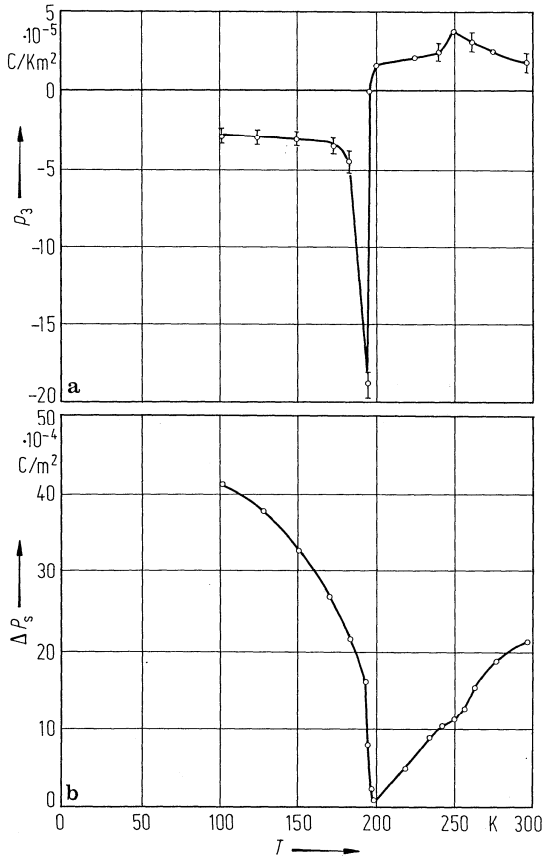

Fig. 41A-2-011. $KLiSO_4$. p_3, ΔP_s vs. T [81Bre]. (**a**) p_3: pyroelectric coefficient on heating. (**b**) ΔP_s: spontaneous polarization change.

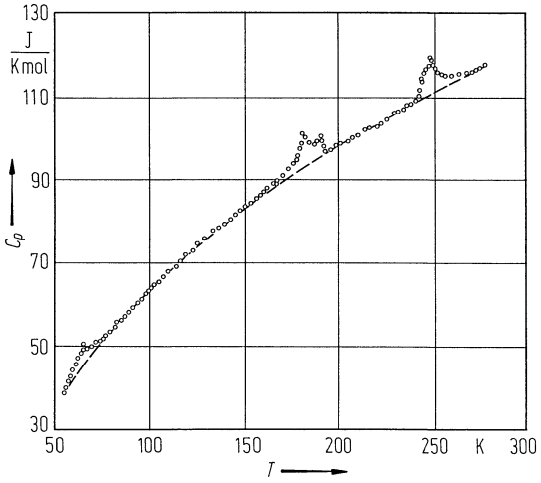

Fig. 41A-2-012. $KLiSO_4$. C_p vs. T [84Isk]. C_p: molar heat capacity at constant pressure.

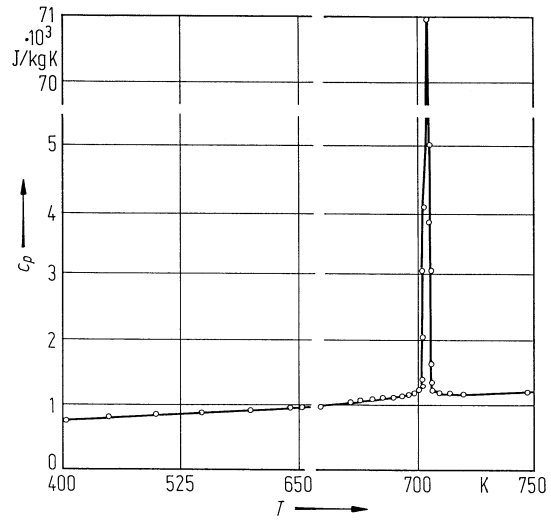

Fig. 41A-2-013. $KLiSO_4$. c_p vs. T [84Bre]. c_p: specific heat capacity at constant pressure.

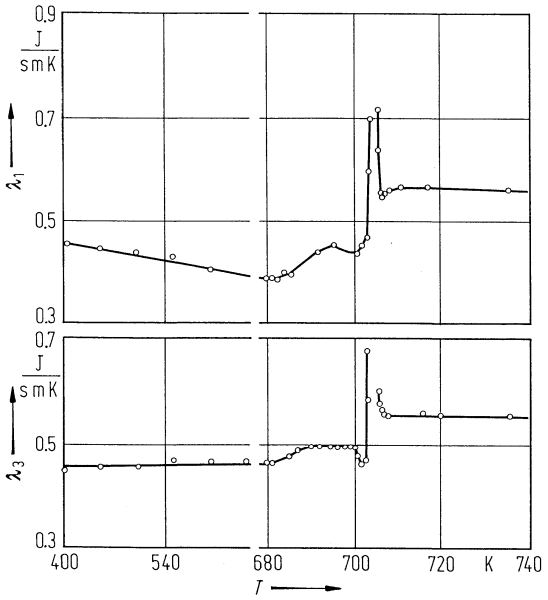

Fig. 41A-2-014. $KLiSO_4$. λ_1, λ_3 vs. T [84Bre]. λ_1 and λ_3: thermal conductivities along the [100] and [001] directions.

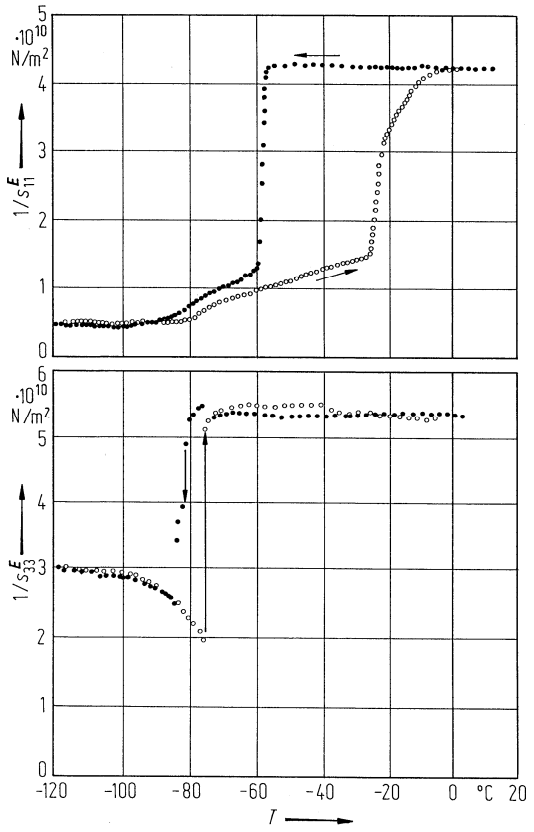

Fig. 41A-2-015. $KLiSO_4$. $1/s_{11}^{\boldsymbol{E}}$ and $1/s_{33}^{\boldsymbol{E}}$ vs. T [85Mae].

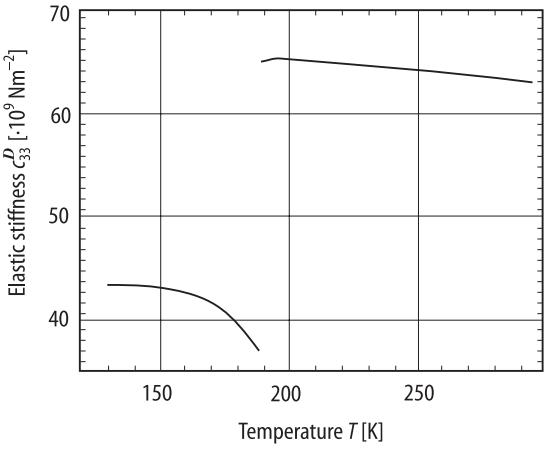

Fig. 41A-2-016. $KLiSO_4$. $c_{33}^{\boldsymbol{D}}$ vs. T [88Kab]. $c_{33}^{\boldsymbol{D}}$: elastic stiffness constant measured under constant D.

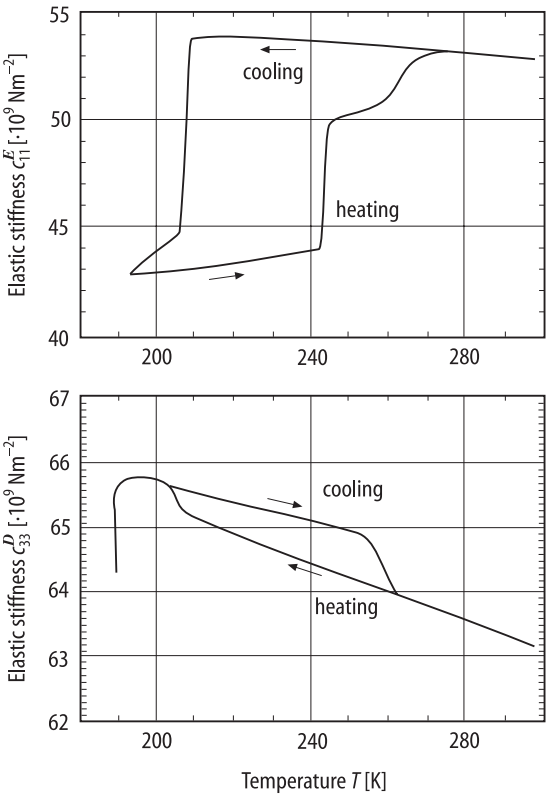

Fig. 41A-2-017. $KLiSO_4$. $c_{11}^{\boldsymbol{E}}$, $c_{33}^{\boldsymbol{D}}$ vs. T [88Kab]. $c_{11}^{\boldsymbol{E}}$: elastic stiffness constant measured under constant E. $c_{33}^{\boldsymbol{D}}$: elastic stiffness constant measured under constant D.

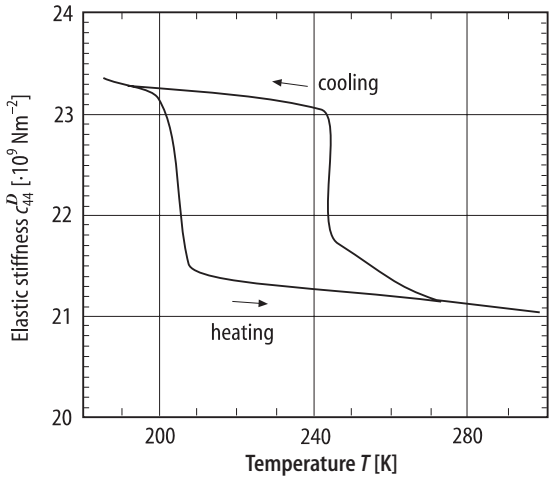

Fig. 41A-2-018. $KLiSO_4$. $c_{44}^{\boldsymbol{D}}$ vs. T [88Kab]. $c_{44}^{\boldsymbol{D}}$: elastic stiffness constant measured under constant D.

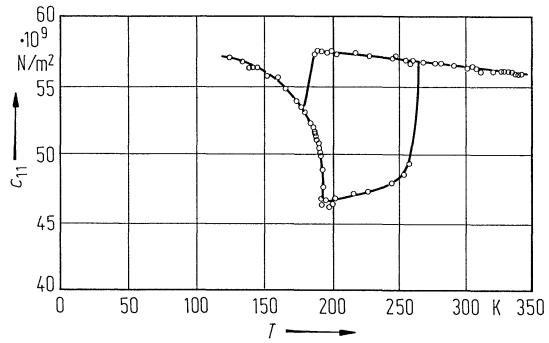

Fig. 41A-2-019. $KLiSO_4$. c_{11} vs. T [85Gan]. c_{11}: elastic stiffness constant determined by Brillouin scattering.

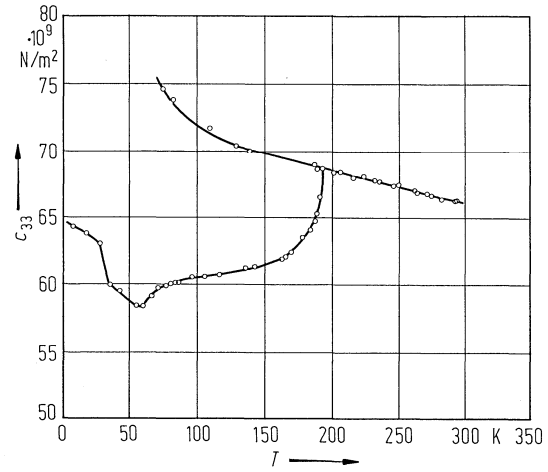

Fig. 41A-2-020. $KLiSO_4$. c_{33} vs. T [85Gan]. Below 190 K, the upper curve corresponds to the unstable high temperature state. c_{33}: elastic stiffness constant determined by Brillouin scattering.

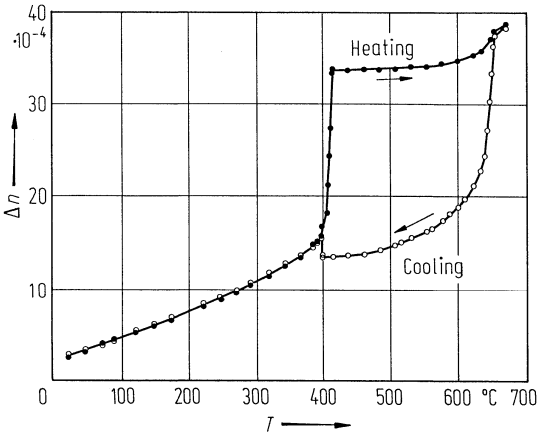

Fig. 41A-2-021. $KLiSO_4$. Δn vs. T [86Zha]. Δn: birefringence for (100) plate at 633 nm.

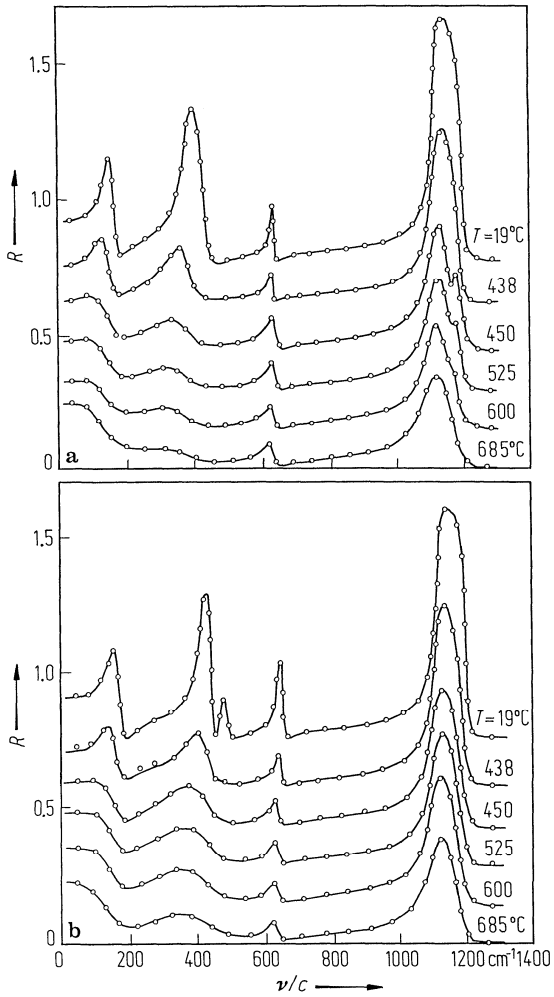

Fig. 41A-2-022. $KLiSO_4$. R vs. ν/c [86Pim]. Parameter: T. R: reflectivity. (**a**) A mode, $E \parallel c$; (**b**) E_1 mode, $E \perp c$.

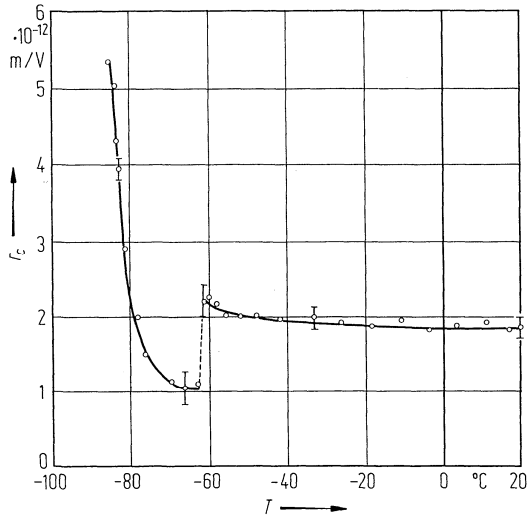

Fig. 41A-2-023. $KLiSO_4$. r_c vs. T [85Fuj2]. $\lambda = 632.8$ nm.

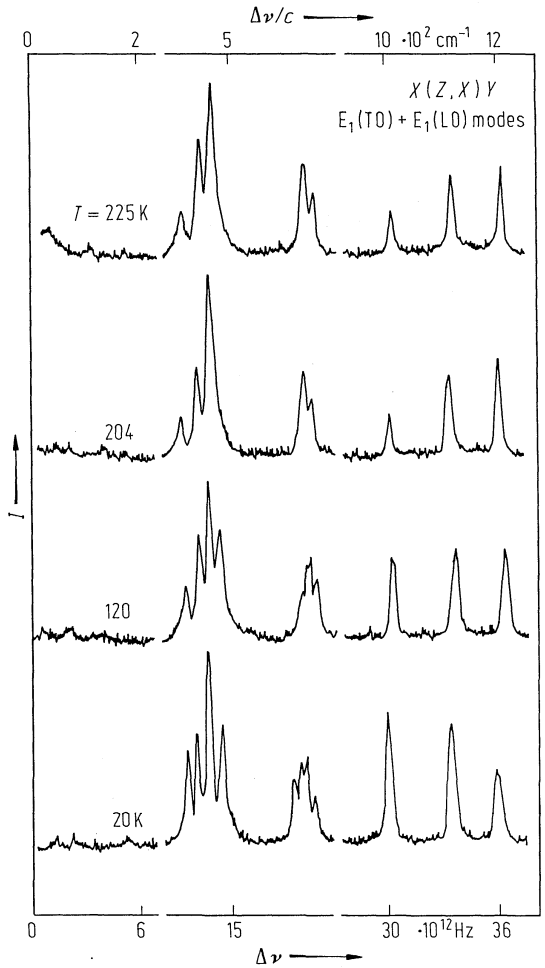

Fig. 41A-2-024. $KLiSO_4$. I vs. $\Delta\nu$ (E_1 modes) [86Men]. I: Raman scattering intensity. Parameter: T.

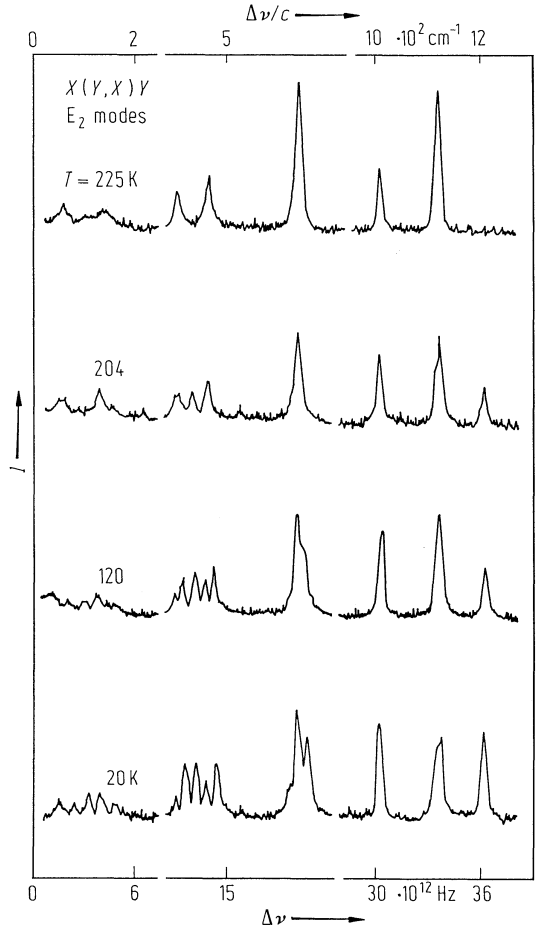

Fig. 41A-2-025. $KLiSO_4$. I vs. $\Delta\nu$ (E_2 modes) [86Men]. I: Raman scattering intensity. Parameter: T.

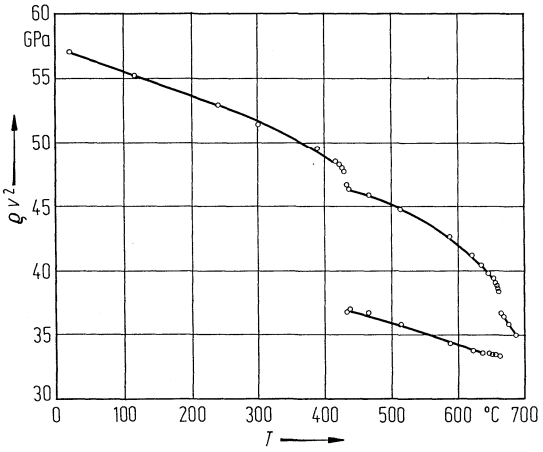

Fig. 41A-2-026. $KLiSO_4$. ρv^2 vs. T [87Pim]. v: velocity of a longitudinal sound wave propagating along the [100] axis. Full lines are guides to the eyes.

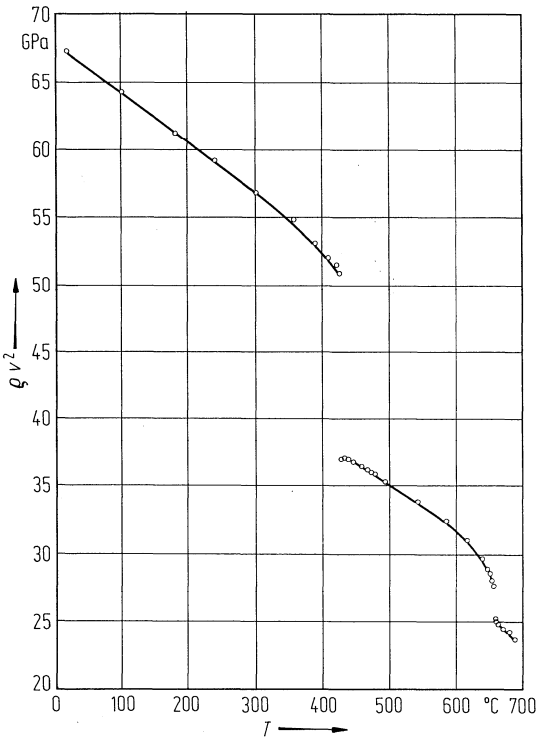

Fig. 41A-2-027. $KLiSO_4$. ρv^2 vs. T [87Pim]. v: velocity of a longitudinal sound wave propagating along the [001] axis. Full lines are guides to the eyes.

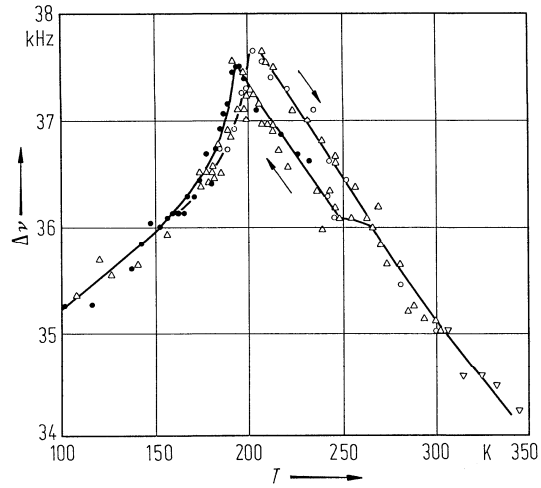

Fig. 41A-2-028. $KLiSO_4$. $\Delta\nu$ vs. T [85Hol]. $\Delta\nu$: frequency separation between satellite lines of ^7Li NMR. $H \parallel c$. ν_L = 34.98 MHz. Each kind of symbols corresponds to a separate experimental run.

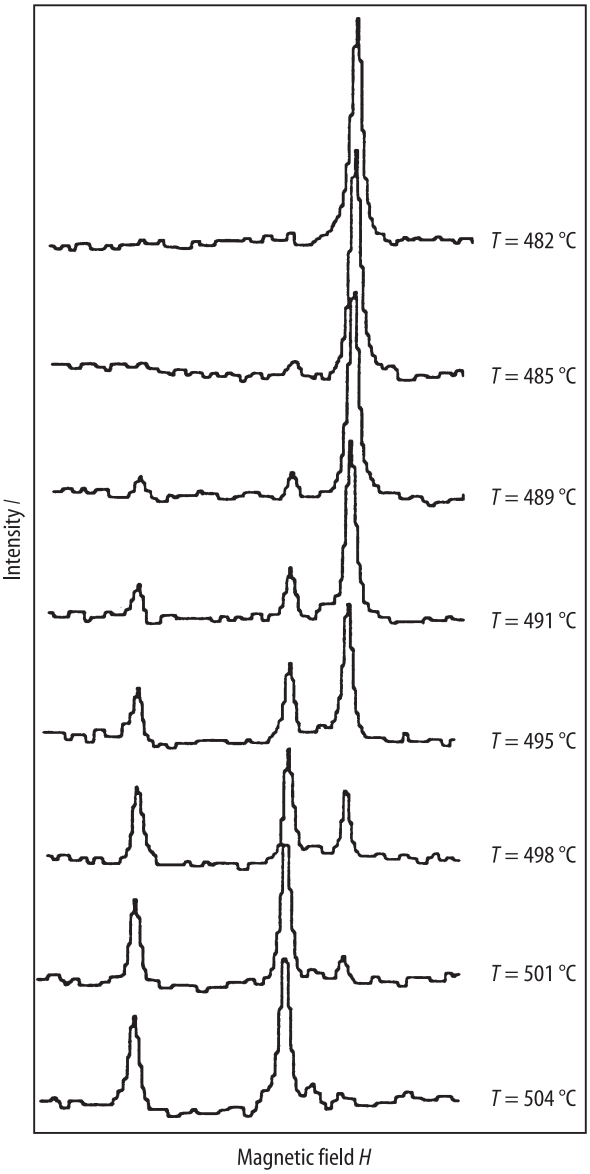

Fig. 41A-2-029. $KLiSO_4$. I vs. H [90Top]. I: intensity of ^{39}K NMR spectra. $H_0 \perp c$, $\angle(H_0, a) = 45°$. Parameter: T.

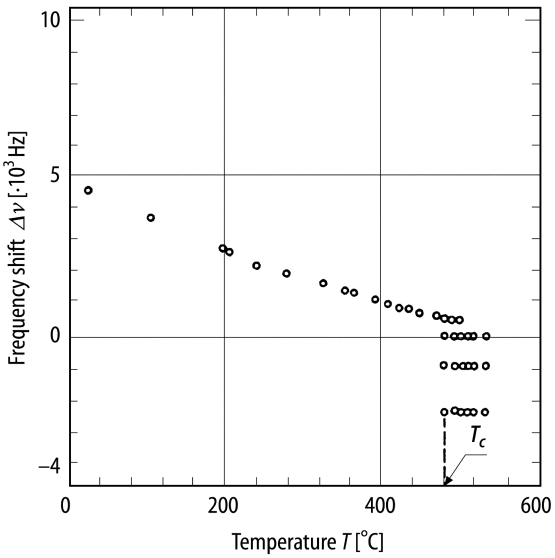

Fig. 41A-2-030. $KLiSO_4$. $\Delta\nu$ vs. T [90Top]. $\Delta\nu$: frequency shift of ^{39}K NMR spectra. $\Delta\nu = \nu - 16.628$ MHz. $H_0 \perp c$, $\angle(H_0, a) = 45°$.

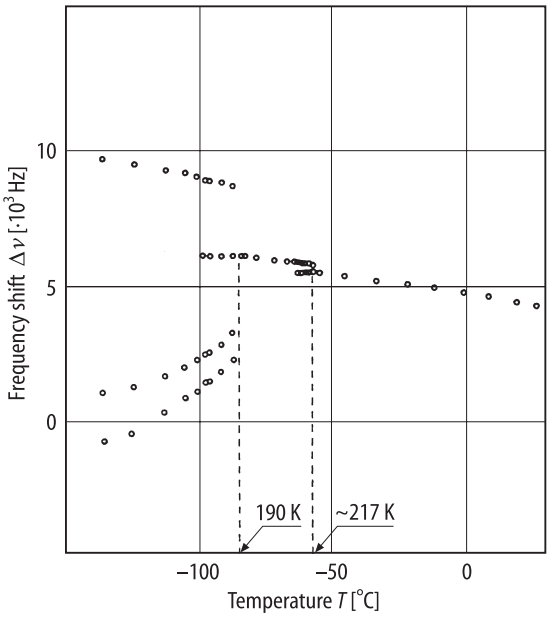

Fig. 41A-2-031. $KLiSO_4$. $\Delta\nu$ vs. T [88Top]. $\Delta\nu$: frequency shift of the second order quadrupole coupling for $H_0 \perp c$. $\theta = 20°$.

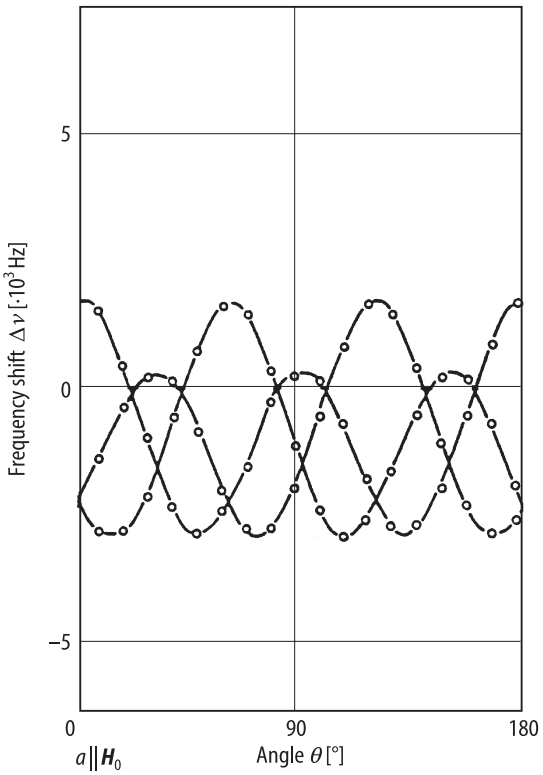

Fig. 41A-2-032. $KLiSO_4$. Δv vs. θ [88Top]. Δv: second order quadrupole shifts of the $^{39}K \pm 1/2 \rightarrow \mp 1/2$ transition for $H_0 \perp c$. $T = 479$ °C.

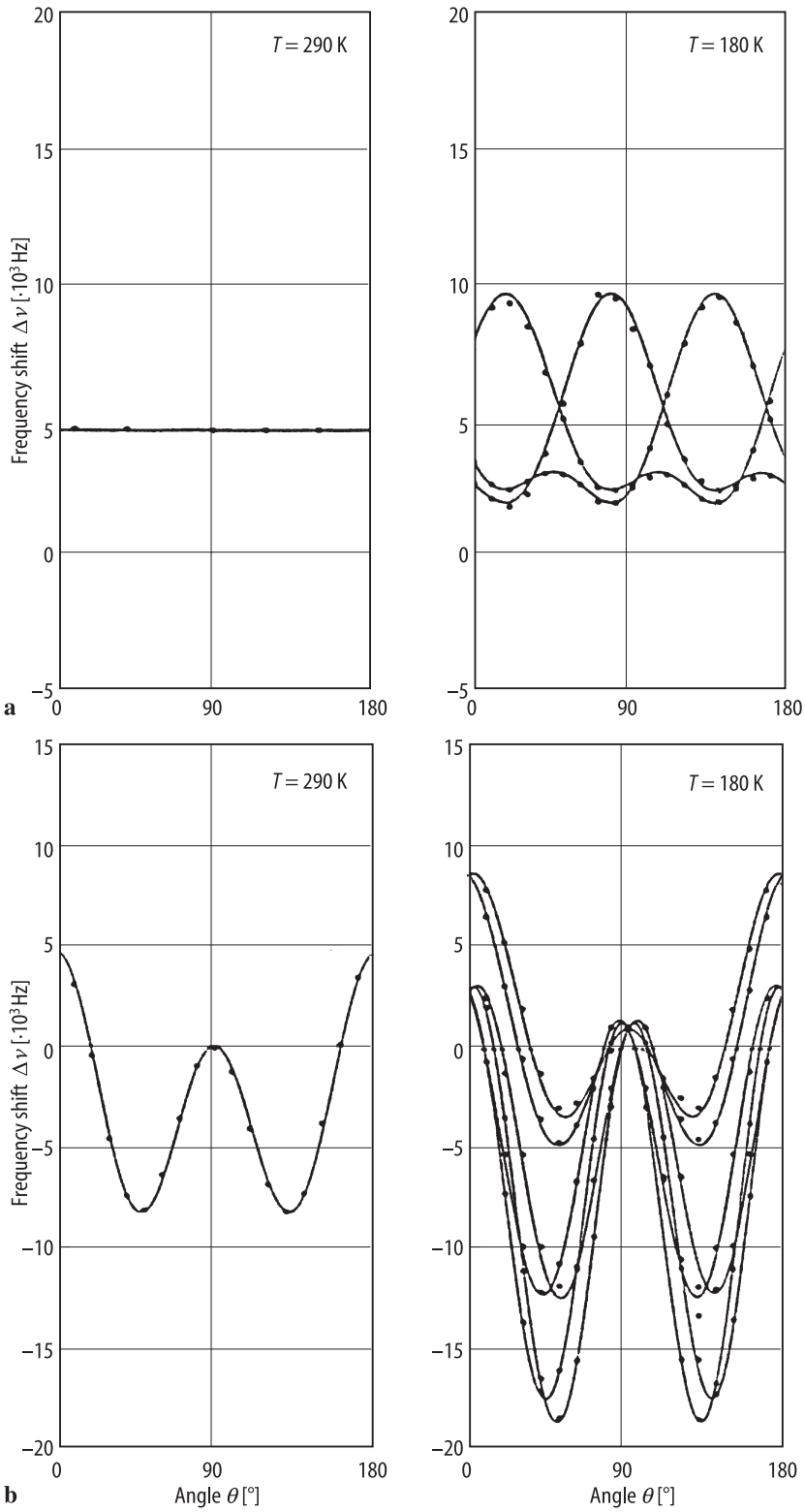

Fig. 41A-2-033. $KLiSO_4$. $\Delta\nu$ vs. θ [88Top]. T = 180, 290 K. $\Delta\nu$: frequency shift of the ^{39}K resonance line for (**a**) $H_0 \perp c$, (**b**) $H_0 \perp a$. $\nu_L = 16.6283 \cdot 10^6$ Hz.

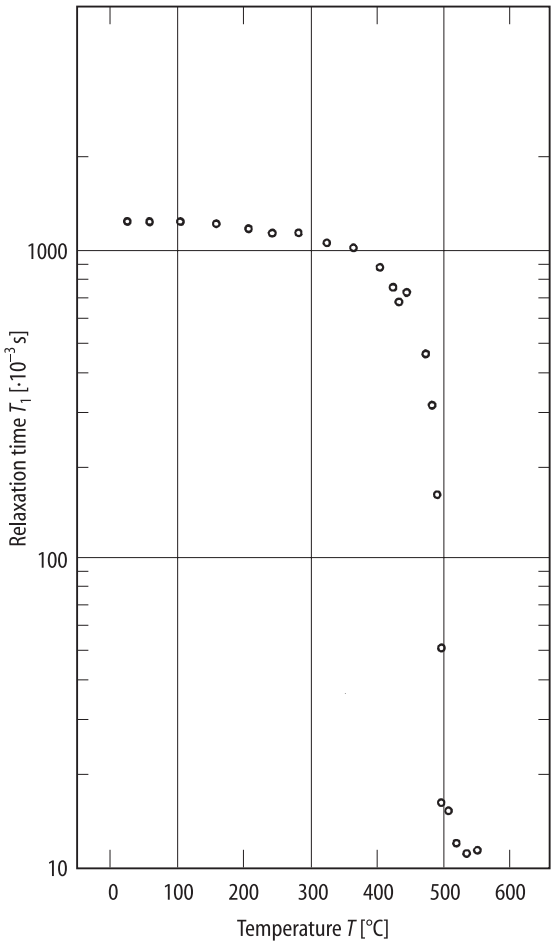

Fig. 41A-2-034. $KLiSO_4$. T_1 vs. T [90Top]. T_1: spin-lattice relaxation time of ^{39}K nucleus. $\nu_L = 16.628 \cdot 10^9$ Hz. $H_0 \perp c$, $\angle(H_0, a) = 45°$.

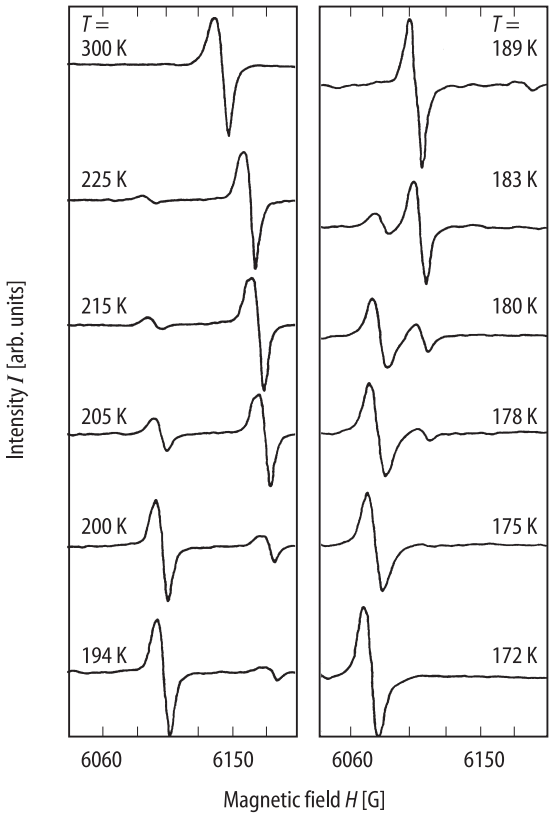

Fig. 41A-2-035. $KLiSO_4$. I vs. H [92Per]. I: intensity of EPR line of Tl^{2+}. $H_0 \parallel c$. Parameter: T.

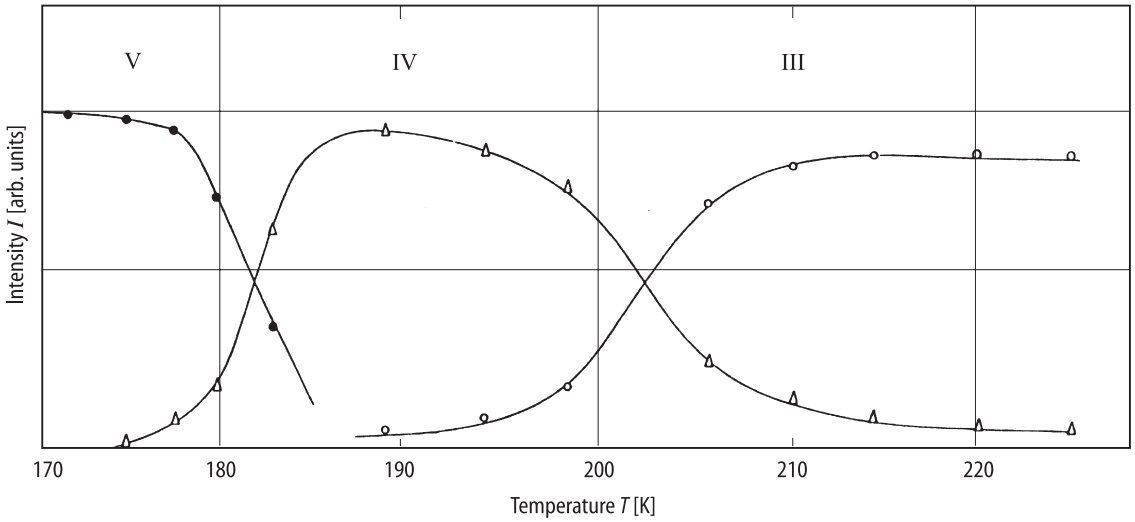

Fig. 41A-2-036. $KLiSO_4$. I vs. T [92Per]. I: intensity of EPR line of Tl^{2+}. $H_0 \parallel c$. Marks, open circle, open triangle and full circle, represent the intensity of the most dominant line in phases III, IV and V, respectively.

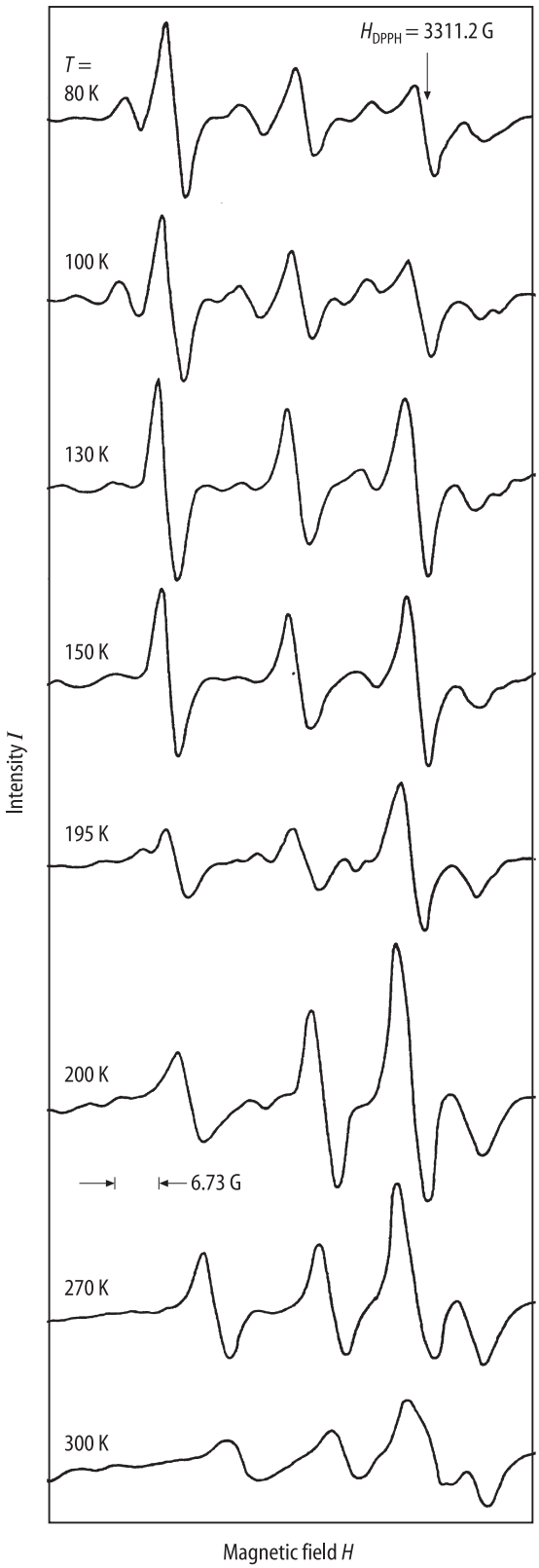

Fig. 41A-2-037. $KLiSO_4$. *I* vs. *H* [87Sas]. *I*: intensity of ESR spectra. Parameter: *T*.

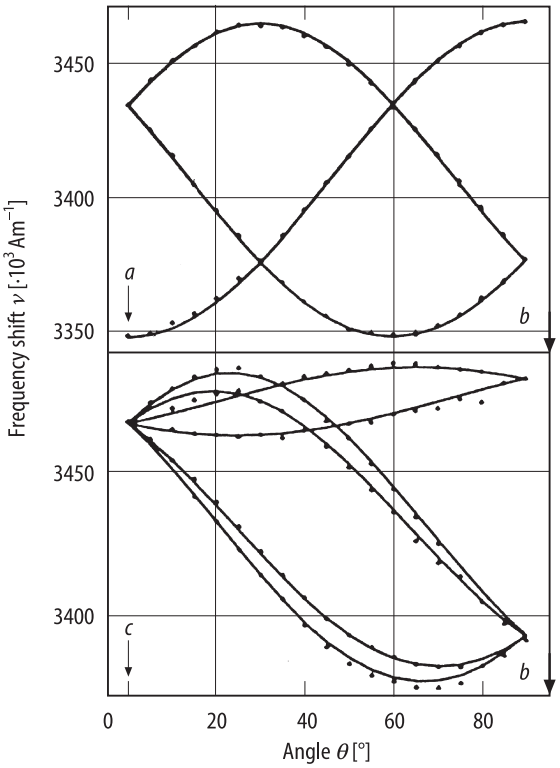

Fig. 41A-2-038. $KLiSO_4$. ν vs. θ [88Bil]. T = 77 K. ν: frequency shift of high-field EPR lines in the *ab* plane and in the *bc* plane.

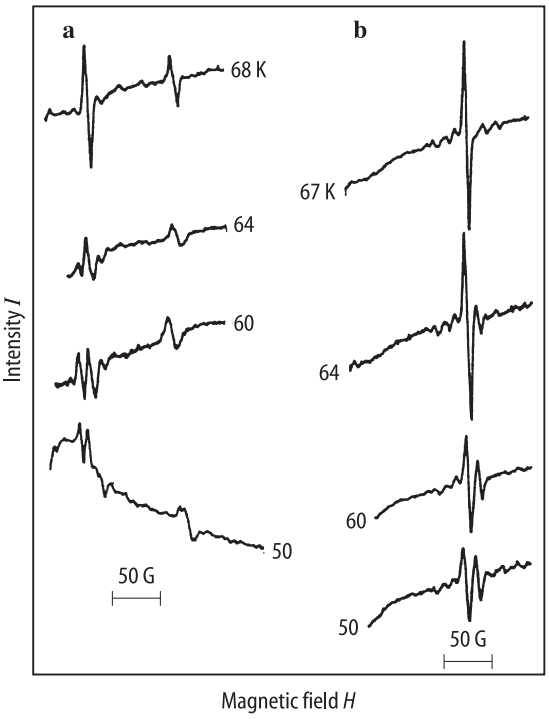

Fig. 41A-2-039. $KLiSO_4$. I vs. H [88Bil]. I: intensity of EPR spectrum observed along the (**a**) *b* axis and (**b**) *c* axis. Parameter: T.

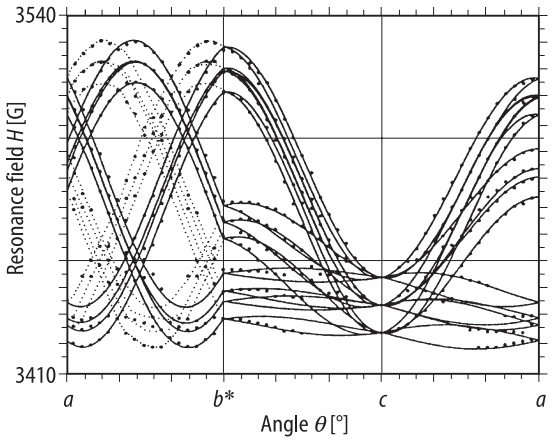

Fig. 41A-2-040. $KLiSO_4$. H vs. θ [93Cho]. T = RT. H: resonance field of EPR line of CrO_4^{3-} in G, 1G = 10^{-4} T. θ: angle between crystal axes and H_0.

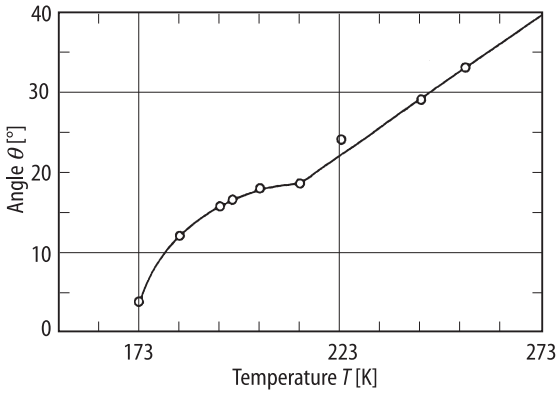

Fig. 41A-2-041. $KLiSO_4$. θ vs. T [87Sas]. θ: amplitude of libration obtained by EPR.

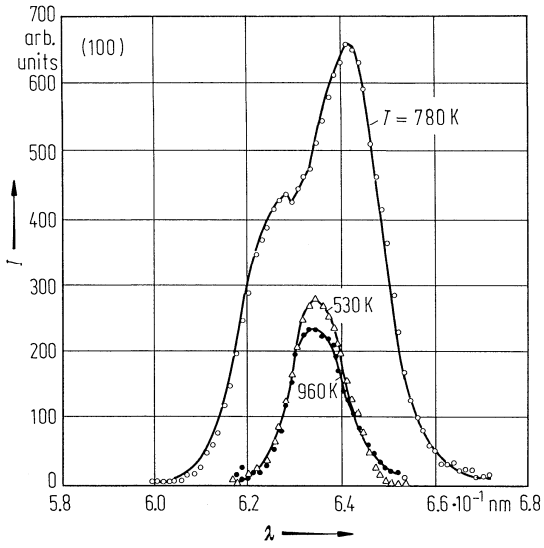

Fig. 41A-2-042. $KLiSO_4$. I vs. λ [86Bal]. I: neutron diffraction intensity of (100) peak. λ: neutron wave length. Parameter: T.

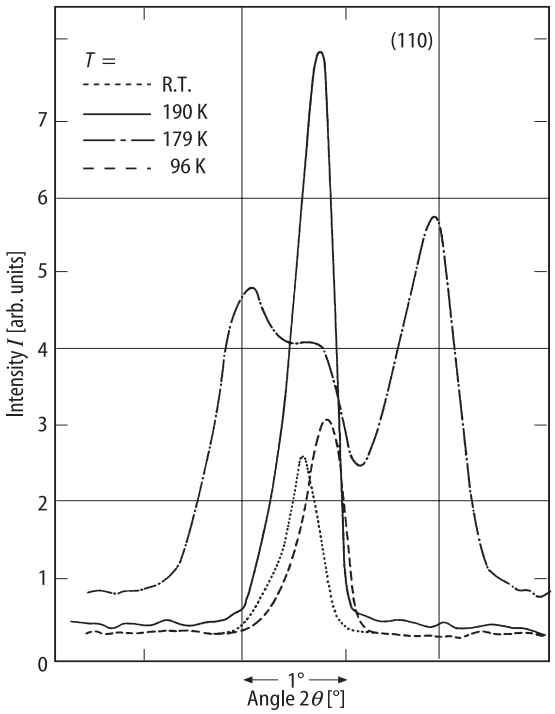

Fig. 41A-2-043. $KLiSO_4$. I vs. 2θ [85Bha]. I: neutron diffraction intensity of (110) peak on cooling run. θ: diffraction angle. Parameter: T.

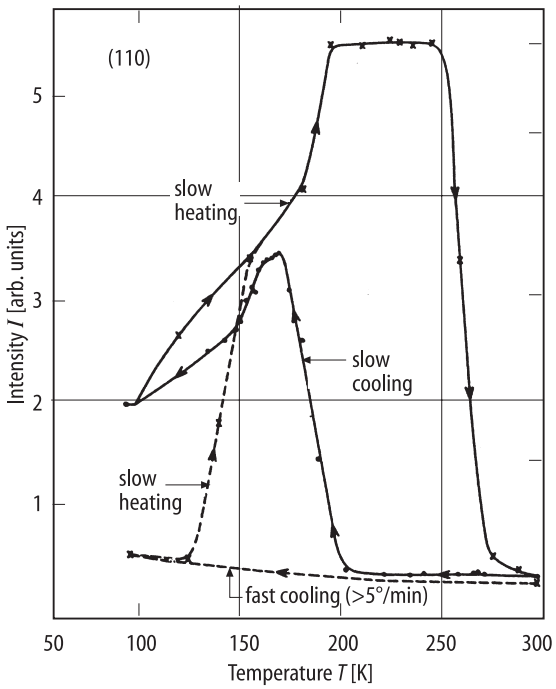

Fig. 41A-2-044. $KLiSO_4$. I vs. T [85Bha]. I: neutron diffraction intensity of (110) peak. Arrows indicate directions of temperature change.

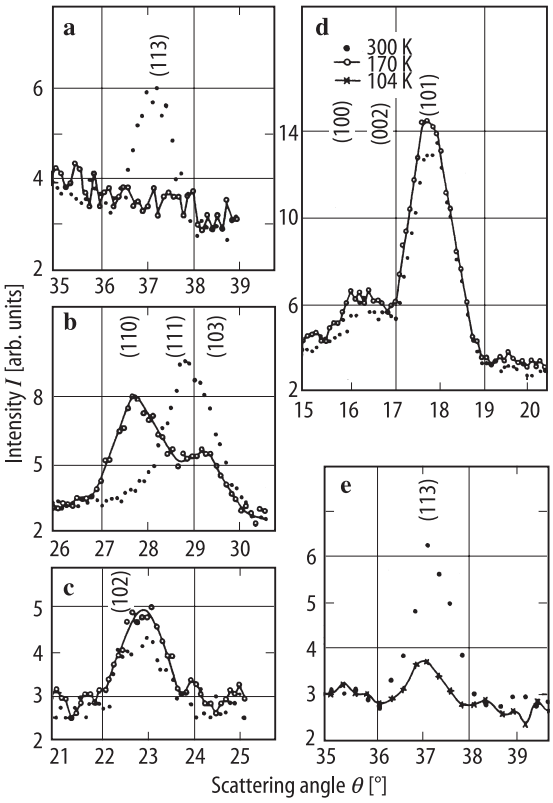

Fig. 41A-2-045. $KLiSO_4$. I vs. θ [85Bha]. I: neutron diffraction intensity of (**a**) (113), (**b**) (110) and (111) (**c**) (102), (**d**) (101), (**e**) (113) peak. Parameter: T.

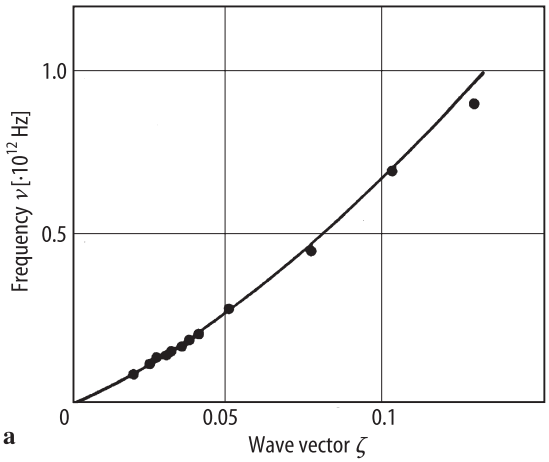

a

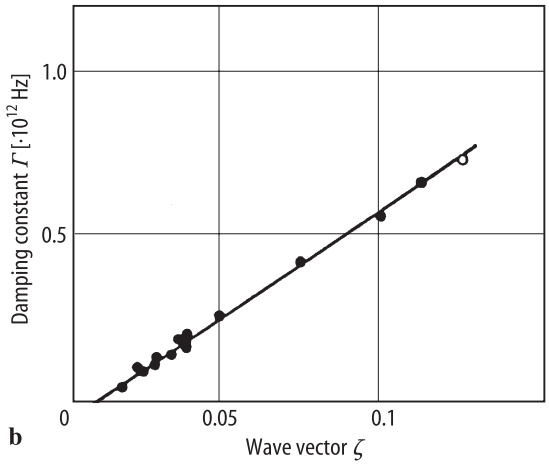

b

Fig. 41A-2-046. $KLiSO_4$. ν, Γ vs. ζ [88Eck]. (**a**) ν: quasiharmonic frequency of transverse acoustic phonon branch along (110) near the Γ point. (**b**) Γ: damping constant of the phonon mentioned above. ζ: wave vector.

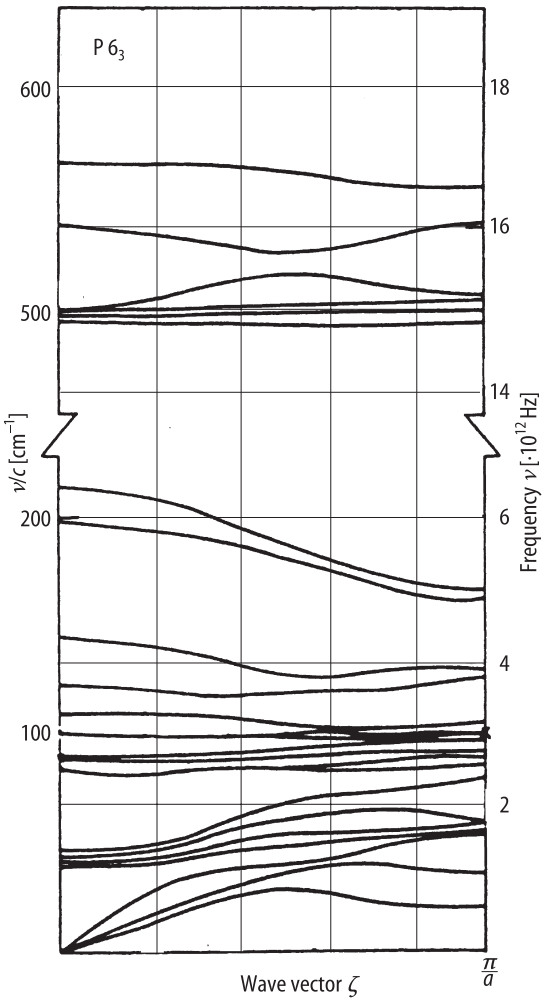

Fig. 41A-2-047. $KLiSO_4$. ν vs. ζ [88Eck]. ν: phonon frequency in phase IV. ζ: wave vector of phonon along the ***a**** axis in the basal plane.

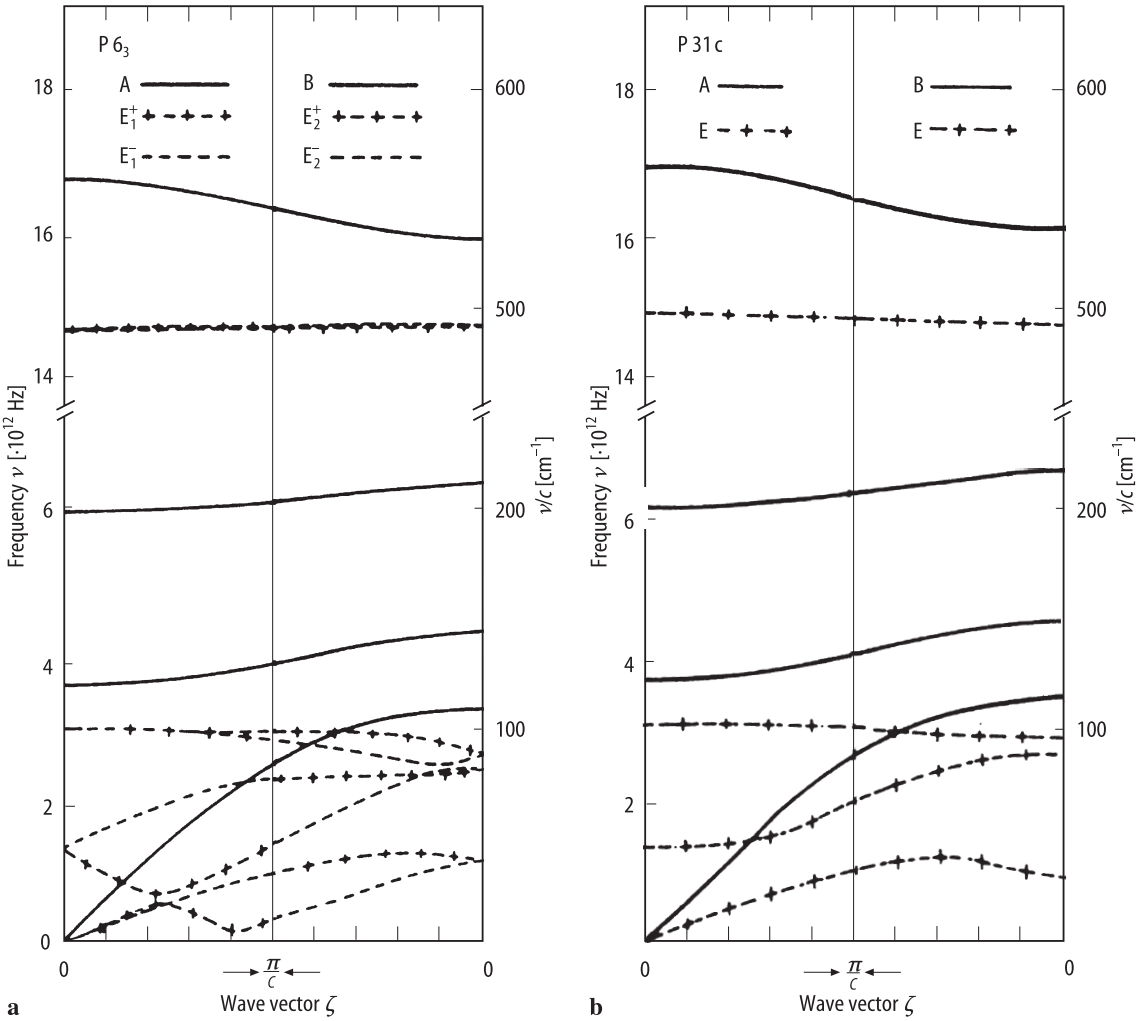

Fig. 41A-2-048. $KLiSO_4$. ν vs. ζ [88Eck]. ν: phonon frequency in (**a**) phase IV and (**b**) phase V. ζ: wave vector of phonon (**a**) along the hexad axis and (**b**) along the c^* axis, respectively.